Desalination and Water Treatment
www.deswater.com

doi: 10.5004/dwt.2023.29899

307 (2023) 30–42
September

Numerical and experimental study of heat and mass transfer in the humidifier of the closed air open water humidification–dehumidification desalination systems

Kien Quoc Vo, Chi Hiep Le*

Department of Heat and Refrigeration, Faculty of Mechanical Engineering, Ho Chi Minh City University of Technology (HCMUT), VNU-HCM, Ho Chi Minh City, Vietnam, emails: lechihiep@hcmut.edu.vn (C.H. Le), vkquoc@hcmut.edu.vn (K.Q. Vo)

Received 18 May 2023; Accepted 21 August 2023

ABSTRACT

This paper presents the findings from a combination of theoretical and experimental investigations into the heat and mass transfer processes within the humidifier of a closed air open water (CAOW) humidification–dehumidification desalination (HDD) system. To develop a theoretical model of the system, heat and mass balance equations were formulated. Subsequently, the effects of input working parameters on output parameters were assessed using a calculation program. Additionally, an experimental model was constructed and tested to evaluate the heat and mass transfer efficiency of the humidifier, which was quantified using the Merkel (Me) number. The investigation into the influence of the input parameters on the output parameters of the humidifier, as facilitated by the theoretical model, was done. The results indicate that the performance of the humidifier is significantly affected by the Me number. Based on the outcomes of the theoretical study, a proposed Me value of approximately 1.6 for the humidifier has been established. Furthermore, it has been demonstrated by the experimental results that the Me number is exclusively dependent on the height of the backing material, the temperature of the spray water, and the mass-flow ratio between water and air. An equation for determining the Me number of the backing material has been formulated based on the experimental and numerical studies on heat and mass transfer inside the humidifier.

Keywords: Runge–Kutta; Heat transfer; Mass transfer; Humidifier; HDD; Desalination

1. Introduction

Humidification–dehumidification desalination (HDD) is a technology utilized to produce fresh water by applying the principle of water evaporating into the air and water condensing from the air. Broadly speaking, the HDD system operates through two main processes: (i) humidification in the humidifier and (ii) dehumidification in the dehumidifier.

In the humidifier, which shares a similar structure with a cooling tower, hot sea water (point 3) is sprayed down onto the packing bed material, while cold air (point 5) is blown up from the bottom. In the closed air and open water (CAOW) HDD cycle, the air entering the humidifier is typically at a saturated state [1–5]. After absorbing both sensible and latent heat from the hot sea water, the air leaves the humidifier at a higher temperature and reaches a new saturated state (point 6). Subsequently, the hot air is directed to the dehumidifier, where it releases some heat to the feed water (point 1) and simultaneously reduces its moisture content. It is then returned to the humidifier to complete the next cycle.

* Corresponding author.

In certain cases, the feed water may not be sufficiently hot, necessitating further heating (point 3) to become the aforementioned hot sea water before entering the humidifier. As the hot sea water evaporates in the humidifier, it leaves the bottom as brine water and is completely removed from the HDD system (point 4). Fig. 1 illustrates the diagram corresponding to the aforementioned working principle of the HDD system.

The performance of the HDD system relies heavily on the moisture content of the air as it leaves the humidifier. The greater the temperature of the air leaving the humidifier, the more moisture it contains. To achieve elevated air temperatures without excessive energy consumption, the heat and mass transfer processes within the humidifier must operate with exceptional efficiency. The arrangement of the humidifier and the specific operational parameters of the water and air play a significant role in influencing these heat and mass transfer processes. To enhance the HDD system's effectiveness, it's essential not only to optimize the operational parameters but also to optimize the humidifier's design. Many studies have been done to make heat and mass transfer work better in humidifiers. The subsequent findings are a result of various studies conducted to investigate heat and mass transfer within HDD systems.

Al-Enezi [6] conducted a study on low-temperature HDD, revealing that the temperature of water entering the humidifier and dehumidifier significantly influences the freshwater yield. The study concluded that higher spray water temperature, lower feed water temperature, and lower mass flow ratio of water and air result in higher heat and mass transfer coefficients. Around the same time, Xiong [7] carried out a theoretical study on the thermally coupled HDD system, introducing a comprehensive mathematical model based on thermodynamic equilibrium to describe the heat and mass transfer processes. The mass transfer coefficient and heat transfer coefficient were determined using correlation relationships. The research findings showed that the calculated mass transfer and heat transfer coefficients, based on correlations and experimental relationships, were in good agreement, with the mass transfer coefficient strongly dependent on air and water flow rates.

In a subsequent study, Amer [8] also conducted a theoretical and experimental investigation of the HDD system, using numerical methods to develop heat and mass balance equations of the system and exploring the influence of working parameters on system performance. The results indicated that the experimentally obtained heat and mass transfer coefficients matched the experimental correlation patterns. Notably, the study revealed that higher water temperature at the humidifier inlet or water flow rate resulted in higher temperature and humidity of the air leaving the humidifier.

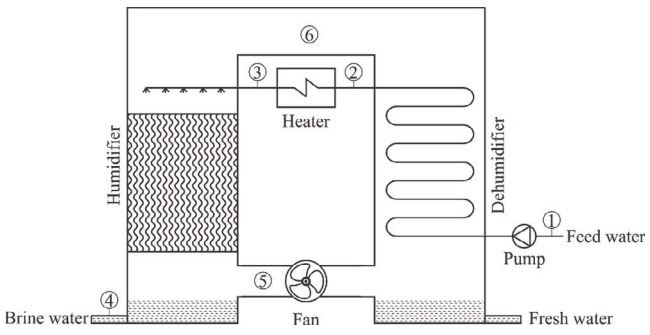

Fig. 1. Diagram of desalination systems by HDD.

Farsad [9] performed an analysis of a solar HDD cycle using the experimental design approach. In this study, the heat and mass balance equations of the humidifier and dehumidifier were solved numerically to analyze the influence of working parameters and freshwater capacity. The outstanding results highlighted the significant impact of mass flow rate and temperature of the feed water, low inlet air, condenser characteristics, and total heat flux on cycle efficiency.

In another nearby study, Hermosillo [10] presented a theoretical and experimental investigation of the HDD system, developing heat and mass balance equations in humidifiers and dehumidifiers to simulate heat transfer and determine steady-state operating temperatures. The published mathematical model effectively simulated heat transfer and calculated the temperature of fluid flows at steady state.

Subsequently, Hamed [11] conducted theoretical and experimental studies on the solar HDD system based on the heat balance of the humidifier and dehumidifier, utilizing a simulation program to evaluate system performance and capacity, with the validation demonstrating its validity under various conditions.

Moumouh [12] also conducted theoretical and experimental studies on the solar-heated HDD system to evaluate its performance through mass and heat balance, along with thermodynamic analysis of the humidifier and dehumidifier. The study led to the development of a mathematical model that showed excellent compatibility with experimental results.

Two years later, Campos [13] conducted a study to evaluate the performance of mathematical models applied in a solar-heated HDD system. The result of this study proposed a more efficient mathematical model to predict freshwater production from seven different models, with estimation of heat and mass transfer coefficients by minimizing the sum of squares of errors of both temperature and distillate predictions. The findings showed that increasing the sprayer height had both beneficial and detrimental effects on desalination yield, with an overall trend of initially increasing clean water output to a certain value and then decreasing it.

Shortly thereafter, Ke [14] presented an experimental and quantitative study of heat and mass transfer in the HDD system's direct humidification. The study revealed a difference of about 12% between theoretical and experimental results. The vapor content of the air leaving the humidifier increased with increasing air flow, spray water temperature, and spray water flow.

Not long after that, Mohamed [15] conducted a theoretical and experimental study of the HDD system, building a mathematical model based on the heat and mass balance of the devices in the cycle to evaluate experimental results. The study demonstrated good agreement between theoretical and experimental work, identifying effective values for the mass flow rate of air, feed water, and spray water.

In the same time, Ahmed [16] also conducted a thermodynamic equilibrium analysis on humidification–dehumidification desalination systems. To enable thermodynamic balancing of HDD desalination systems, a numerical model was introduced. In this study, the correlation between temperature and specific enthalpy of saturated air in the HDH model was simplified. The analytical and numerical outcomes were compared to those of prior studies, demonstrating the reliability and accuracy of the proposed approaches.

Also, during this time, Yin [17] also conducted a numerical investigation on a heat pump-powered HDD system. In this study, a mathematical model was developed based on the heat and mass balance equations for each component and then validated using experimental data. The study focused on examining the impact of key parameters related to the air and seawater entering the system on its overall performance. Through parametric analysis, it was observed that air temperature had a minimal effect on system productivity. However, increasing the air humidity ratio or seawater flow rate positively contributed to enhancing the system's yield. Additionally, the yield demonstrated variations with increasing seawater temperature.

Next after that, Damson [18] conducted a comprehensive investigation into the HDD process, utilizing a combination of numerical and experimental simulations to assess and enhance system performance. In this study, a novel mechanical model for the HDD system was introduced, supplanting conventional models. The mechanical model was developed by converting the heat and mass transfer equations at the water-air interface into enthalpy equations. The study's findings revealed that the proposed model exhibited a mean square error of approximately 0.4.

Recently, Saidi [19] conducted a comprehensive investigation involving both numerical and experimental approaches to analyze a solar-powered humidification–dehumidification desalination device. The desalination device was mathematically modeled, incorporating heat and mass balance principles. To handle the equations effectively, the finite difference method was employed, and MATLAB software proved instrumental in solving these complex mathematical expressions. The results of the study show the compatibility between numerical and experimental methods.

Merkel was the first to propose a method for analyzing and calculating the heat and mass transfer processes in a cooling tower, with certain assumptions made to simplify the calculations. The Merkel method ignores the effect of the amount of water evaporating into the air in the heat balance equation and sets the Lewis factor being equal to 1. Many of the aforementioned studies have focused on developing mathematical models based on the Merkel method. However, the results obtained in these studies have not yet evaluated the heat and mass transfer efficiency in the humidifier. While cooling towers share similarities with humidifiers in principle, there are also differences, particularly in the state of the working fluid within the system. Thus, applying the cooling tower calculation theory directly to the humidifier may not be appropriate.

In contrast to the Merkel method, the Poppe method takes into account the effect of the amount of water evaporating into the air and the Lewis factor as well. However, so far there have been very few theoretical studies on the HDD system using the Poppe method, and there has been no any numerical simulation using the Poppe method for the HDD system.

Based on the aforementioned summarization, the aim of this study is to ascertain the suitable Me number for enhancing the heat and mass transfer efficiency within the humidifier. This study delves out the heat and mass transfer mechanism within the humidifier of the HDD system using Poppe's numerical method [20]. Subsequently, a comprehensive numerical simulation program was developed to assess the impact of operational parameters on the heat and mass transfer processes within the humidifier. Moreover, to establish an equation that demonstrates the connection between operational parameters, packing bed height within the humidifier, and the Me number, an experimental model was also constructed to appraise the influence of operational parameters and packing bed height on the humidifier's mass transfer coefficient.

From the simulation results, experimental studies will be carried out to determine the relationship between mass flow rate ratio, packing bed height and Me number.

The process of heat and mass transfer in the humidifier depends on these parameters:

- Temperature of spraying water;
- Temperature of air enter the humidifier;
- Mass flow rate ratio (m);
- Dimension of the humidifier: area of spray surface, material of packing bed, height of packing bed.

2. Theoretical model

The process of heat and mass transfer in the humidifier is illustrated in Fig. 2. Initially, the incoming hot water has a flow rate of $\dot{m}_w$ and an enthalpy of $Cp_w(t_w + dt_w)$. Subsequently, after undergoing the heat and mass transfer with air, the water exits with a flow rate of $\dot{m}_w - d\dot{m}_w$ and an enthalpy of $Cp_w t_w$. Likewise, the incoming air has a flow rate of $\dot{m}_a(1 + w_a)$ and an enthalpy of h_a, while the exiting air has a flow rate of $\dot{m}_a(1 + w_a + dw_a)$ and an enthalpy of $h_a + dh_a$.

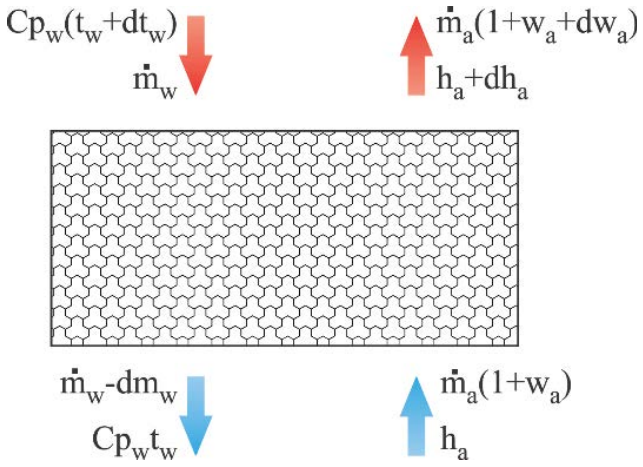

Fig. 2. Process of mass and heat transfer in the humidifier.

Assumptions: To formulate the heat and mass balance equations for the humidifier, the following assumptions are taken into account: [21–23]

- The convective heat loss outside the wall of the humidifier is ignored.
- The mass transfer is uniform by the height (*dz*) of the packing bed.
- The cross-section of the packing bed in the direction of motion in the humidifier is uniform.
- The air pressure is constant.
- The relative humidity of circulating air in the humidifier as 100%.

2.1. Mass and heat balance in the humidifier

Mass balance:

$$\dot{m}_w + \dot{m}_a\left(1 - w_a\right) = \dot{m}_a\left(1 + w_a + dw_a\right) + \dot{m}_w - d\dot{m}_w \tag{1}$$

where $\dot{m}_w$ – kg of water vapour/s, $\dot{m}_a$ – kg of dry air/s, w_a – kg of water vapour/kg of dry air (Abbreviation as: kg/kg).

Rearranging the Eq. (1):

$$\dot{m}_a dw_a = d\dot{m}_w \tag{2}$$

Heat balance equation:

$$\dot{m}_a \mathrm{Cp}_w\left(t_w + dt_w\right) + \dot{m}_a h_a = \dot{m}_a\left(h_a + dh_a\right) + \left(\dot{m}_w - d\dot{m}_w\right)\mathrm{Cp}_w t_w \tag{3}$$

Rearranging the Eq. (3):

$$\dot{m}_a dh_a - d\dot{m}_w \mathrm{Cp}_w t_w - \dot{m}_w \mathrm{Cp}_w dt_w = 0 \tag{4}$$

Substituting Eq. (2) to Eq. (4):

$$dt_w = \frac{\dot{m}_a}{\dot{m}_w \mathrm{Cp}_w}\left(dh_a - dw_a \mathrm{Cp}_w t_w\right) \tag{5}$$

Enthalpy of saturated air:

$$\begin{aligned} h_a &= \mathrm{Cp}_a t_a + w_a\left(r_w + \mathrm{Cp}_v t_a\right) = \mathrm{Cp}_a t_a + w_a\left(h_v - \mathrm{Cp}_v t_w + \mathrm{Cp}_v t_a\right) \\ &= \mathrm{Cp}_a t_a + w_a h_v - w_a \mathrm{Cp}_v\left(t_w - t_a\right) \end{aligned} \tag{6}$$

$$\begin{aligned} h_{\mathrm{sa}} &= \mathrm{Cp}_a t_w + w_{\mathrm{sa}}\left(r_w + \mathrm{Cp}_v t_w\right) \\ &= \mathrm{Cp}_a t_w + w_{\mathrm{sa}}\left(h_v - \mathrm{Cp}_v t_w + \mathrm{Cp}_v t_w\right) = \mathrm{Cp}_a t_w + w_{\mathrm{sa}} h_v \end{aligned} \tag{7}$$

$$\begin{aligned} h_{\mathrm{sa}} - h_a &= \left(t_w - t_a\right)\left(\mathrm{Cp}_a + w_a \mathrm{Cp}_v\right) \\ &+ w_{\mathrm{sa}} h_v - w_a h_v \rightarrow t_w - t_a = \frac{\left(h_{\mathrm{sa}} - h_a\right) - \left(w_{\mathrm{sa}} - w_a\right)h_v}{\mathrm{Cp}_a + w_a \mathrm{Cp}_v} \end{aligned} \tag{8}$$

The mass flow of spray water evaporating into the air:

$$d\dot{m}_w = K_M\left(w_{\mathrm{sa}} - w_a\right)dA \tag{9}$$

From Eq. (2) and Eq. (9):

$$dw_a = \frac{K_M\left(w_{\mathrm{sa}} - w_a\right)dA}{\dot{m}_a} \tag{10}$$

The total heat transferring to the air:

$$dQ_a = dQ_c + dQ_m = \dot{m}_a dh_a \tag{11}$$

where:

The sensible heat:

$$dQ_c = \dot{m}_a \mathrm{Cp}_a dt_a = \alpha_{\mathrm{sa}}\left(t_w - t_a\right)dA \tag{12}$$

The latent heat:

$$dQ_m = h_v \dot{m}_a dw_a = h_v K_M\left(w_{\mathrm{sa}} - w_a\right)dA \tag{13}$$

$$\rightarrow dQ_a = \alpha_{\mathrm{sa}}\left(t_w - t_a\right)dA + h_v K_M\left(w_{\mathrm{sa}} - w_a\right)dA \tag{14}$$

Substituting Eq. (8) to Eq. (14):

$$\rightarrow dQ_a = \left[\begin{array}{l} \alpha_{\mathrm{sa}}\dfrac{\left(h_{\mathrm{sa}} - h_a\right)}{\left(\mathrm{Cp}_a + w_a \mathrm{Cp}_v\right)K_M} - \\ \left(\dfrac{\alpha_{\mathrm{sa}}}{\left(\mathrm{Cp}_a + w_a \mathrm{Cp}_v\right)K_M} - 1\right)h_v\left(w_{\mathrm{sa}} - w_a\right) \end{array}\right] K_M dA \tag{15}$$

The Lewis factor [24]:

$$\mathrm{Le} = \frac{\alpha_{\mathrm{sa}}}{\left(\mathrm{Cp}_a + w_a \mathrm{Cp}_v\right)K_M} \tag{16}$$

According to Bosnjakovic [25], the The Lewis factor in cooling towers is:

$$\mathrm{Le} = 0.865^{0.667}\frac{\left(\dfrac{w_{\mathrm{sa}} + 0.622}{w_a + 0.622} - 1\right)}{\ln\left(\dfrac{w_{\mathrm{sa}} + 0.622}{w_a + 0.622}\right)}$$

$$dh_a = \frac{K_M dA}{\dot{m}_a}\left[\mathrm{Le}\left(h_{\mathrm{sa}} - h_a\right) - \left(\mathrm{Le} - 1\right)\left(w_{\mathrm{sa}} - w_a\right)h_v\right] \tag{17}$$

$$dA = aVdz$$

where:

$$\mathrm{Me} = \frac{K_M \cdot a \cdot V}{\dot{m}_w} \text{ is the Me number [26]} \tag{18}$$

$$dh_a = m\mathrm{Me}\left[\mathrm{Le}\left(h_{\mathrm{sa}} - h_a\right) - \left(1 - \mathrm{Le}\right)\left(w_{\mathrm{sa}} - w_a\right)h_v\right]dz \tag{19}$$

From Eq. (10):

$$dw_a = m \cdot \mathrm{Me}\left(w_{\mathrm{sa}} - w_a\right)dA \tag{20}$$

Substituting Eqs. (9) and (17) to Eq. (4):

$$\dot{m}_w dh_w = K_M dA\left[\begin{array}{l} h_{\mathrm{sa}} - h_a + \left(\mathrm{Le} - 1\right)\left(h_{\mathrm{sa}} - h_a - \left(w_{\mathrm{sa}} - w_a\right)h_v\right) \\ -\left(w_{\mathrm{sa}} - w_a\right)\mathrm{Cp}_w t_w \end{array}\right] \tag{21}$$

From Eq. (5):

$$\frac{dw_a}{dt_w} = \frac{dh_a}{t_w dh_w} - \frac{\dot{m}_w}{t_w \dot{m}_a} \tag{22}$$

Substituting Eq. (17) and (21) to Eq. (22):

$$\frac{dw_a}{dt_w}=\frac{\dot{m}_w}{\dot{m}_a}\left[\frac{\mathrm{Cp}_w\left(w_{\mathrm{sa}}-w_a\right)}{h_{\mathrm{sa}}-h_a+\left(\mathrm{Le}-1\right)\left[h_{\mathrm{sa}}-h_a-\left(w_{\mathrm{sa}}-w_a\right)h_v\right]}-\left(w_{\mathrm{sa}}-w_a\right)\mathrm{Cp}_w t_w\right] \tag{23}$$

Substituting Eq. (22) to Eq. (23):

$$\frac{dh_a}{dt_w}=\mathrm{Cp}_w\frac{\dot{m}_w}{\dot{m}_a}\left[1+\frac{\mathrm{Cp}_w t_w\left(w_{\mathrm{sa}}-w_a\right)}{h_{\mathrm{sa}}-h_a+\left(\mathrm{Le}-1\right)\left(h_{sa}-h_a-\left(w_{\mathrm{sa}}-w_a\right)h_v\right)-\left(w_{\mathrm{sa}}-w_a\right)\mathrm{Cp}_w t_w}\right] \tag{24}$$

From Eqs. (2) and (9):

$$K_M dA=\frac{\dot{m}_a dw_a}{\left(w_{\mathrm{sa}}-w_a\right)} \tag{25}$$

Rearranging the Eq. (25):

$$\frac{K_M dA}{\dot{m}_w}=\frac{\dot{m}_a\dfrac{dw_a}{dt_w}}{\dot{m}_w\left(w_{\mathrm{sa}}-w_a\right)}dt_w \tag{26}$$

Integrating Eq. (26):

$$\int\frac{K_M dA}{\dot{m}_w}=\int\frac{\dot{m}_a\dfrac{dw_a}{dt_w}}{\dot{m}_w\left(w_{\mathrm{sa}}-w_a\right)}dt_w \tag{27}$$

$$\mathrm{Me}=\frac{K_M A}{\dot{m}_w}=\int\frac{\dot{m}_a\dfrac{dw_a}{dt_w}}{\dot{m}_w\left(w_{\mathrm{sa}}-w_a\right)}dt_w$$

According to Poppe's approach, Eq. (27) is also called the Me number.

Substituting Eq. (23) to Eq. (27):

$$\frac{d\mathrm{Me}}{dt_w}=\frac{\mathrm{Cp}_w}{h_{\mathrm{sa}}-h_a+\left(\mathrm{Le}-1\right)\left(h_{\mathrm{sa}}-h_a\left(w_{\mathrm{sa}}-w_a\right)h_v\right)-\left(w_{\mathrm{sa}}-w_a\right)\mathrm{Cp}_w t_{\boldsymbol{w}}} \tag{28}$$

In the humidifier, mass transfer takes place between the spray water and the air. This process is represented in the following equation:

$$\dot{m}_{\mathrm{wi}}=\dot{m}_w+\dot{m}_a\left(w_o-w\right) \tag{29}$$

$$\rightarrow\frac{\dot{m}_w}{\dot{m}_a}=\frac{\dot{m}_{\mathrm{wi}}}{\dot{m}_a}\left(1-\frac{\dot{m}_a}{\dot{m}_{\mathrm{wi}}}\left(w_o-w\right)\right) \tag{30}$$

2.2. Methodology

During mass transfer, there is an increase in the enthalpy and vapor content of the air, while the temperature of the spray water decreases. These parameters are interdependent and influence each another. The relationships between these parameters can be expressed through the following functions:

$$\frac{dw_a}{dt_w}=f_1\left(t_w,h_a,w_a\right) \tag{31}$$

$$\frac{dh_a}{dt_w}=f_2\left(t_w,h_a,w_a\right) \tag{32}$$

$$\frac{d\mathrm{Me}}{dt_w}=f_3\left(t_w,h_a,w_a\right) \tag{33}$$

To solve the differential equations, the 4th order Runge–Kutta method is used. According to the Runge–Kutta method, the parameters in the division interval are determined according to the following formula:

$$w_{a(n+1)}=w_{a(n)}+\frac{\left(j_{(n+1,1)}+2j_{(n+1,2)}+2j_{(n+1,3)}+j_{(n+1,4)}\right)}{6} \tag{34}$$

$$h_{a(n+1)}=h_{a(n)}+\frac{\left(k_{(n+1,1)}+2k_{(n+1,2)}+2k_{(n+1,3)}+k_{(n+1,4)}\right)}{6} \tag{35}$$

$$\mathrm{Me}_{(n+1)}=\mathrm{Me}_{(n)}+\frac{\left(l_{(n+1,1)}+2l_{(n+1,2)}+2l_{(n+1,3)}+l_{(n+1,4)}\right)}{6} \tag{36}$$

Where:

$$j_{(n+1,1)}=\Delta t_w.f_1\left(t_{w(n)},h_{a(n)},w_{a(n)}\right) \tag{37}$$

$$k_{(n+1,1)}=\Delta t_w.f_2\left(t_{w(n)},h_{a(n)},w_{a(n)}\right) \tag{38}$$

$$l_{(n+1,1)}=\Delta t_w.f_3\left(t_{w(n)},h_{a(n)},w_{a(n)}\right) \tag{39}$$

$$j_{(n+1,2)}=\Delta t_w.f_1\left(t_{w(n)}+\frac{\Delta t_w}{2},h_{a(n)}+\frac{k_{(n+1,1)}}{2},w_{a(n)}+\frac{j_{(n+1,1)}}{2}\right) \tag{40}$$

$$k_{(n+1,2)}=\Delta t_w.f_2\left(t_{w(n)}+\frac{\Delta t_w}{2},h_{a(n)}+\frac{k_{(n+1,1)}}{2},w_{a(n)}+\frac{j_{(n+1,1)}}{2}\right) \tag{41}$$

$$l_{(n+1,2)}=\Delta t_w.f_3\left(t_{w(n)}+\frac{\Delta t_w}{2},h_{a(n)}+\frac{k_{(n+1,2)}}{2},w_{a(n)}+\frac{j_{(n+1,1)}}{2}\right) \tag{42}$$

$$j_{(n+1,3)}=\Delta t_w.f_1\left(t_{w(n)}+\frac{\Delta t_w}{2},h_{a(n)}+\frac{k_{(n+1,2)}}{2},w_{a(n)}+\frac{j_{(n+1,2)}}{2}\right) \tag{43}$$

$$k_{(n+1,3)} = \Delta t_w . f_2\left(t_{w(n)} + \frac{\Delta t_w}{2}, h_{a(n)} + \frac{k_{(n+1,2)}}{2}, w_{a(n)} + \frac{j_{(n+1,2)}}{2}\right) \quad (44)$$

$$l_{(n+1,3)} = \Delta t_w . f_3\left(t_{w(n)} + \frac{\Delta t_w}{2}, h_{a(n)} + \frac{k_{(n+1,2)}}{2}, w_{a(n)} + \frac{j_{(n+1,2)}}{2}\right) \quad (45)$$

$$j_{(n+1,4)} = \Delta t_w . f_1\left(t_{w(n)} + \Delta t_w, h_{a(n)} + k_{(n+1,3)}, w_{a(n)} + j_{(n+1,3)}\right) \quad (46)$$

$$k_{(n+1,4)} = \Delta t_w . f_2\left(t_{w(n)} + \Delta t_w, h_{a(n)} + k_{(n+1,3)}, w_{a(n)} + j_{(n+1,3)}\right) \quad (47)$$

$$l_{(n+1,4)} = \Delta t_w . f_3\left(t_{w(n)} + \Delta t_w, h_{a(n)} + k_{(n+1,3)}, w_{a(n)} + j_{(n+1,3)}\right) \quad (48)$$

3. Experimental setup

The experimental setup is illustrated in Figs. 3 and 4. The humidifier features a square cross-section measuring 30 cm on each side and is constructed from 304 stainless steel. Standing at a height of 220 cm, the humidifier is divided into compartments, each with a height of 15 cm, providing space for layers of packing bed material. The packing bed material utilized in the humidifier is cooling pad paper, boasting a total surface area per unit volume of approximately 640 m^2/m^3.

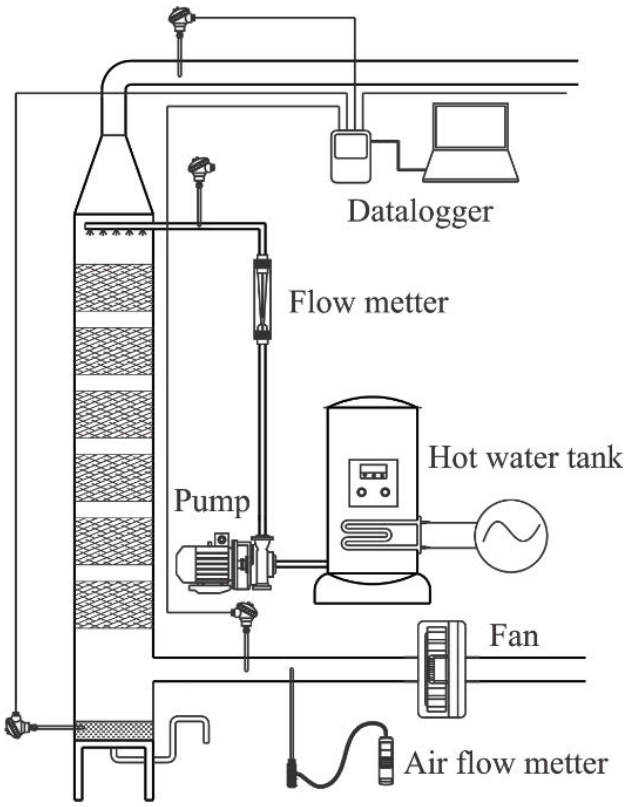

Fig. 3. Experimental model.

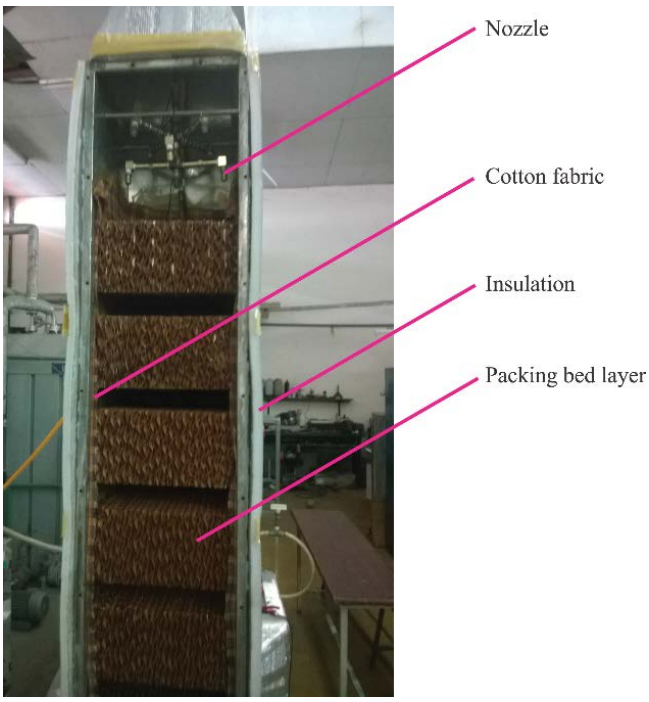

Fig. 4. Structure of humidifier.

The height of the cooling pad layers within the humidifier can be adjusted by altering the number of layers of packing material, and there exists a 5 cm gap between each layer. Positioned on the top of the humidifier are nine nozzles, evenly spaced out. To mitigate the water's velocity along the walls, a thin layer of woven cotton coats the interior of the humidifier. On the ou tside, the humidifier is insulated with a 2 cm-thick layer of insulating material.

To measure the flow rate of hot water, float-type flowmeters were employed, offering a range of 0.02–15 L/min and an accuracy of ±4%. For air flow measurement, an anemometer (Testo 425) was used, with a scale of 1–12 m/s and an accuracy of ±0.1%. Temperature data was logged using a Testo 176T4 data logger, boasting an accuracy of ±0.3°C and a resolution of 0.1°C, to monitor the temperature of both water and air at the inlet and outlet of the humidifier.

To control the temperature of the spray water which is in fact sea water with the salinity of 26 g/L, a 300-L water tank heated by 2 resistors providing a total output of 18 kW and an accuracy of ±2°C was employed.

A hot water pump with a capacity of 750 W, a flow rate of 3.4 m^3/h, and a head of 52 mH_2O was used to supply water to the humidifier. To regulate the spray water flow, a bypass was implemented to return excess water to the water tank.

For the air supply to the humidifier, a centrifugal fan with a capacity of 65 W, a flow rate of 300 m^3/h, and a head of 350 Pa was utilized. To maintain the temperature of the air entering the humidifier, a water-cooled dehumidifier was employed.

4. Results and discussions

Using the principles of Runge–Kutta analysis, a simulation program has been developed with fixed input

parameters, including the spray water temperature, air temperature, and Me number.

In the previous research findings [27], it was observed that with a minimum temperature difference of 3°C–5°C between water and air, the optimal spray water temperature ranged from 66°C–74°C. Corresponding to this optimum spray water temperature, the optimal mass flow ratio falls within the range of 2.5–3.5. Hence, for this study, the spray water temperature and mass flow rate will be chosen to be within the intervals of 60°C–80°C and m in the range of 1–4, respectively.

4.1. Effect of m on the temperatures of water and air leaving the humidifier

Fig. 5 illustrates the impact of m and spray water temperature (t_3) on the temperature of water leaving the humidifier (t_4) at an entering air temperature of 35°C and Me number of 1.2. The findings reveal that t_4 shows a linear variation with m, and as t_3 increases, t_4 also rises. However, the difference in t_4 resulting from the difference in t_3 is relatively small, and as t_3 increases further, the difference in t_4 diminishes.

The Me number is directly proportional to the mass transfer coefficient and the contact surface area, while inversely proportional to the spray water flow. Consequently, a higher flow rate (m) leads to an increased spray water flow. With a constant Me number, as the spray water flow rises, both the mass transfer coefficient and the contact surface area also increase, resulting in greater heat exchange between water and air. Nevertheless, this exchange of heat does not increase proportionally with the spray water flow, leading to a decrease in the difference between water temperature at the inlet and outlet of the humidifier as m increases. In that case, t_4 will increase while t_3 remains constant.

Fig. 6 illustrates the impact of spray water temperature (t_3) and m on the temperature of air leaving the humidifier (t_6) while maintaining a constant Me number and inlet air temperature (t_5). The results indicate that t_6 increases with m, but the relationship is not linear; instead, it follows a curved pattern. Higher t_3 values correspond to higher t_6 values. However, the variation in t_6 with m is not consistent across different t_3 values. As t_3 increases, the difference in t_6 resulting from changes in m becomes more pronounced.

Interestingly, the trends of t_6 and t_4 with m at different spray water temperatures are opposite. As the value of m increases, the variations in t_4 and t_6 in relation to t_3 tend to diverge.

Similarly, it can be explained that t_6 increases as m increases, as described above in the change of t_4 with m. When the spray water flow increases, the heat exchange between water and air intensifies, leading to an increase in t_6 while t_5 remains constant. Due to the exchange of latent and sensible heat between air and water, the variation in t_6 is not linear with m.

4.2. Effect of Me number

The results presented in Fig. 7 reveal the impact of Me number on the temperature of water leaving the humidifier. It is evident that, at a constant value of m, t_4 t_4 varies inversely with the Me number. However, the rate of t_4 decrease is not uniform with the rate of Me increase; t_4 shows significant variation with Me in the low range, while its changes are gradual in the high range. Additionally, as the Me number increases, t_4 becomes almost unchanged with variations in t_3. The Me number is directly proportional to the heat and mass transfer area, and inversely proportional to the spray water flow. This result clearly indicates the impact of both mass transfer area and spray water flow on the performance of the humidifier. A higher Me number, indicating a larger mass transfer area or a lower spray water flow, leads to enhanced heat and mass transfer efficiency, resulting in a lower t_4. Moreover, a higher Me number indicates a more efficient humidifier. However, the efficiency of the humidifier increases slowly when the mass transfer area is excessively large. From these results, it is also evident that the higher the m, the higher the t_4.

Fig. 8 illustrates the impact of the Me number on the temperature of air leaving the humidifier (t_6) while maintaining a constant spray water temperature (t_3) and the air temperature entering the humidifier (t_5). The results reveal that t_6 increases positively with the Me number, consistent with the variation observed in t_4 as discussed earlier. The Me number represents the efficiency of heat and mass transfer in a humidifier. A higher Me number indicates a more effective heat and substance transfer process, resulting in increased heat exchange, higher t_6, and lower t_4. However, the rate of increase is not uniform; it is faster in the range

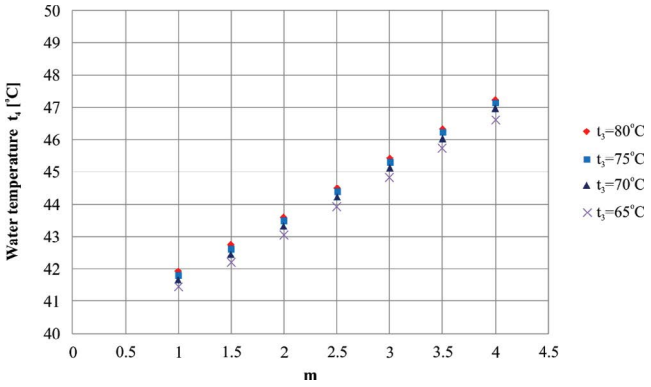

Fig. 5. Effect of m on the temperature of water leaving the humidifier at Me = 1.2 and t_5 = 35°C.

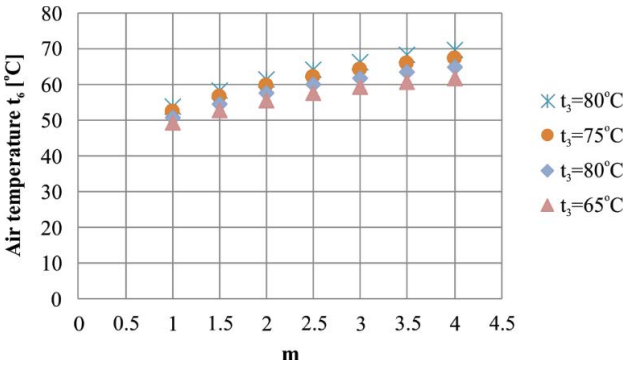

Fig. 6. Effect of m on the temperature of air leaving the humidifier at Me = 1.2 and t_5 = 35°C.

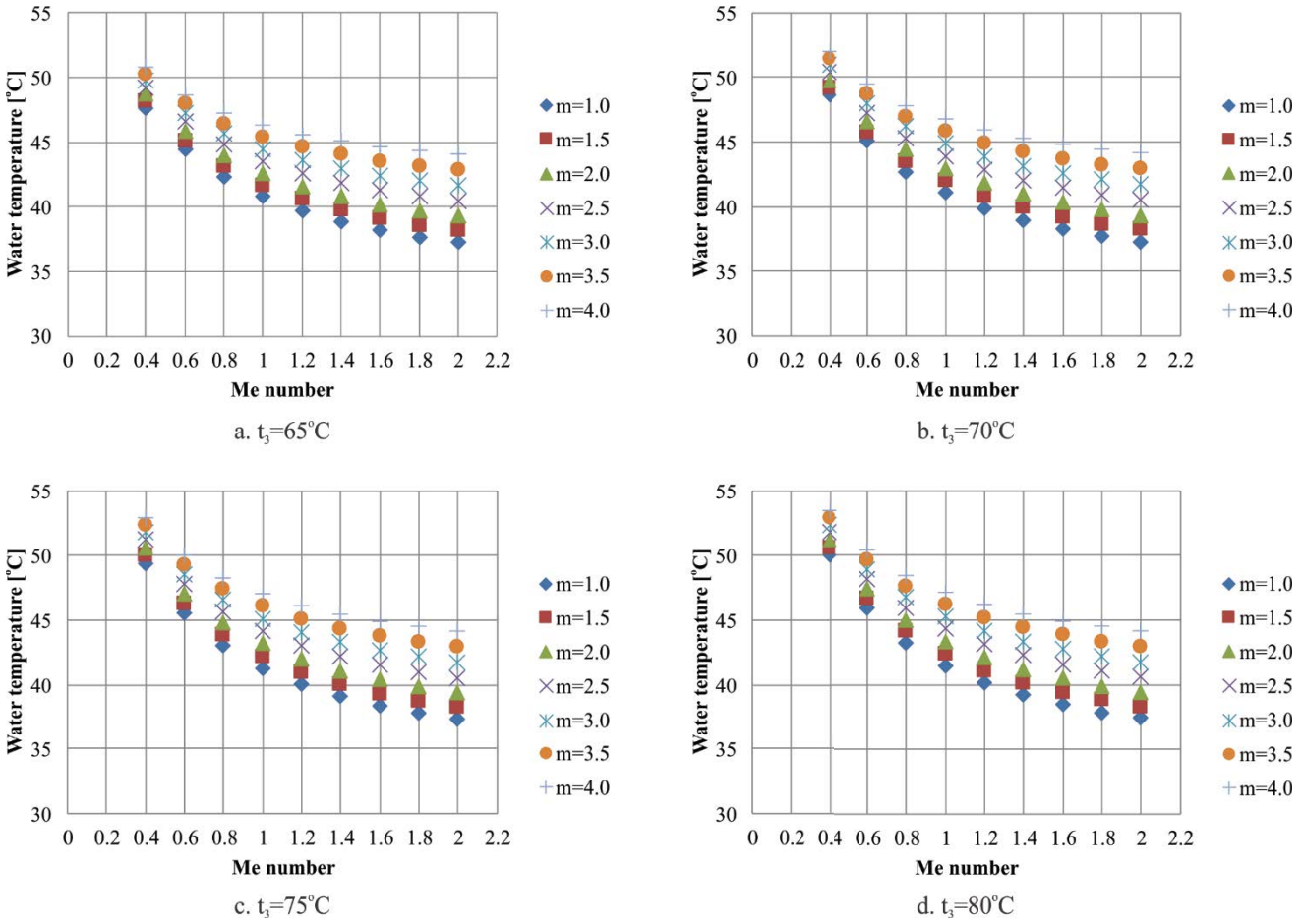

Fig. 7. Effect of Me number on temperature of water leaving the humidifier at t_5 = 35°C.

of Me = 0.4–1.2. Subsequently, from Me number values of 1.2 to 1.6, t_6 increases at a slower rate, and for Me > 1.6, t_6 experiences a very gradual increase. Consequently, it can be concluded that the suitable Me number for designing a humidifier is Me = 1.6.

The results in Fig. 9 indicate that the temperature of air entering the humidifier has a minor impact on the temperature of water and air leaving the humidifier. The effect is relatively small for t_4 and insignificant for t_6. This can be easily understood because in the humidifier, the water and air circulate in opposite directions, and the air entering the humidifier comes into contact with the water leaving the humidifier. As a result, t_4 is more influenced by t_5. From these findings, it is evident that t_6 and t_4 depend heavily on t_3, the Me number, and m, but not significantly on t_5.

4.3. Simulation error analysis

In order to assess the precision of the simulation results, an error analysis was conducted while altering the input parameters Me, m, and t_3. The outcomes of this error analysis are displayed in Tables 1–3. The error analysis involves confirmation through the energy balance equation. The findings of the analysis reveal that the simulation program's maximum error stands at nearly 1.23%, a relatively minor deviation. This serves as evidence that the simulation program is highly dependable.

4.4. Experimental results

Experimental results indicate the temperature of spray water and the temperature of air leaving the humidifier only. Therefore, the evaluation of heat and mass transfer in the humidifier is very complicated and difficult. So that, to evaluate the heat and mass transfer in the humidifier, the Me number is used. The Me number is a non-dimensional parameter and cannot be measured by experimental method. In this paper, the Me number is determined by combining of theoretical and experimental results.

4.5. Effect of entering air temperature on Me number

The air entering the humidifier is the same air that exits the dehumidifier. The temperature of the air entering the humidifier is influenced by the cooling water temperature in the dehumidifier. However, the temperature of the air entering the humidifier only changes within a narrow range. To assess the impact of the entering air temperature on heat and

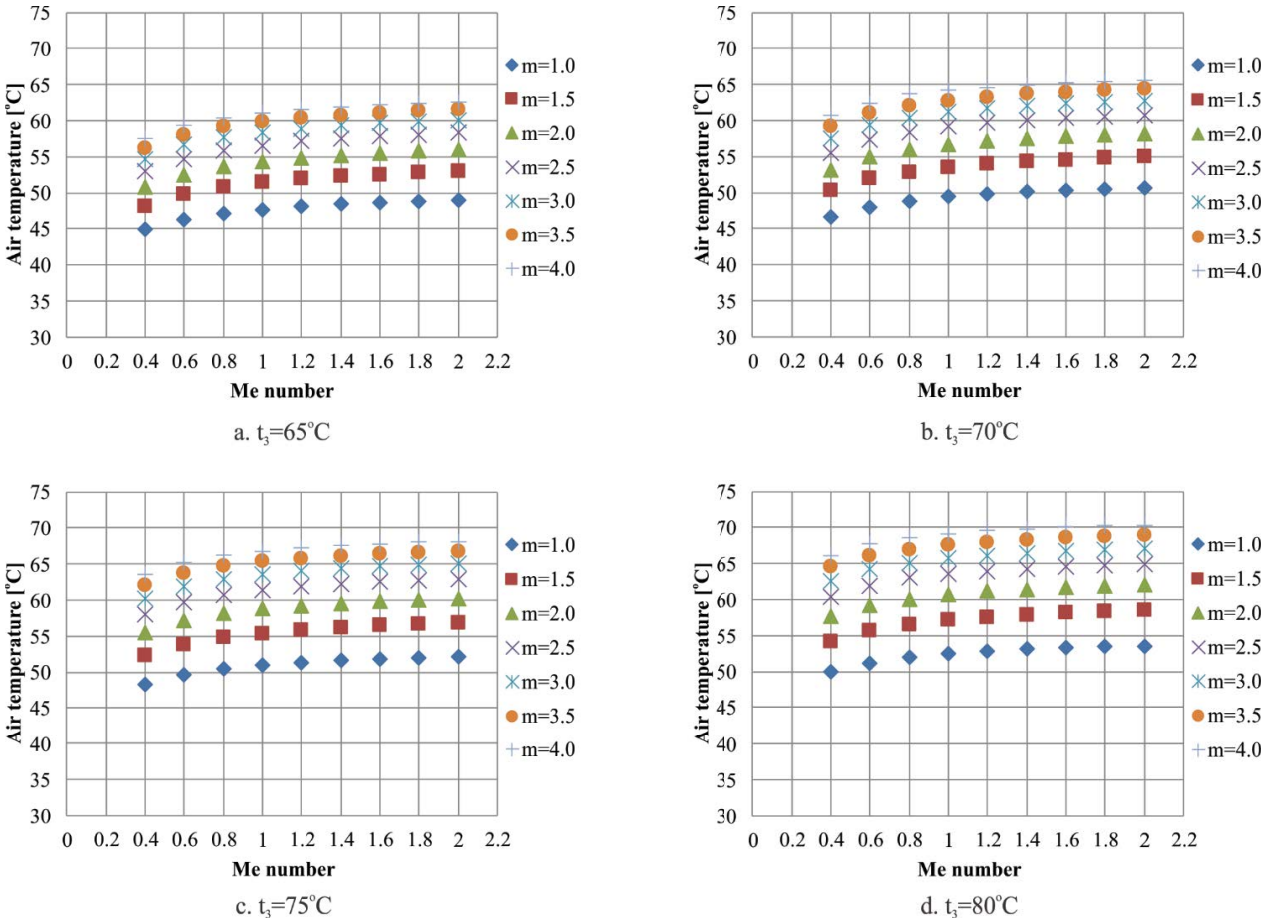

Fig. 8. Effect of Me number on temperature of air leaving the humidifier at t_5 = 35°C.

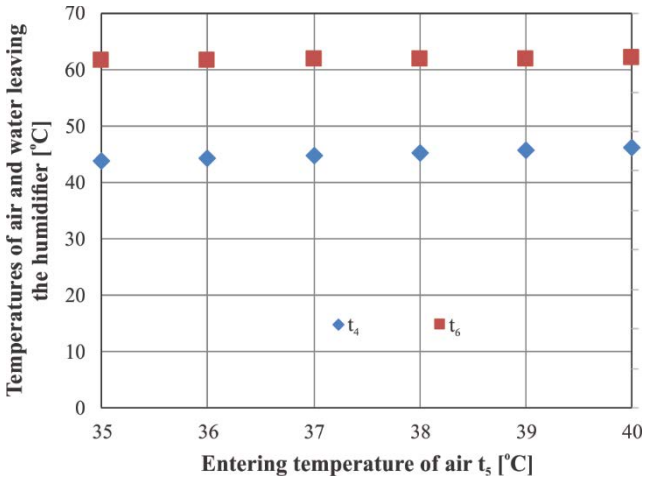

Fig. 9. Effect of temperature of air entering the humidifier on temperatures of air and water leaving the humidifier at Me = 1.2 and t_3 = 70°C.

mass transfers in the humidifier, an experimental study was conducted. The study involved varying the temperature of the air entering the humidifier and analyzing the resulting changes in the temperatures of the air and water leaving the humidifier.

Fig. 10 illustrates the impact of the air temperature entering the humidifier on the temperatures of the air and water leaving the humidifier, with a spray water temperature of 75°C, packing bed height (L) of 1.2 m, and a mass flow rate ratio (m) between the spray water and air set at 3.5. The experimental results align well with the theoretical results conducted earlier. The temperature of water leaving the humidifier exhibits a linear change with the temperature of the entering air, while the temperature of air leaving the humidifier shows almost no significant change.

Using a simulation program, the Me number was calculated based on the experimental data. The simulation results indicate that the Me number remains constant regardless of the temperature of the air entering the humidifier. This finding suggests that in the CAOW-HDD system, the entering air temperature of the humidifier does not significantly impact the heat and mass transfer processes. Consequently, to eliminate an independent variable in the regression equation, the temperature of the air entering the humidifier will be kept constant in the experiments.

4.6. *Effect of spray water temperature on Me number*

The spray water temperature significantly influences the convective heat transfer coefficient and the mass transfer coefficient in the humidifier, as well as the Me

Table 1
Simulation error vs. Merkel number Me

Me	m	t_3 (°C)	t_6 (°C)	t_4 (°C)	t_5 (°C)	Q_i (W)	Q_0 (W)	Error (%)
0.4	2	80	35	51.22	57.599	903.7248	899.3736	0.48147
0.6	2	80	35	47.44	59.16	903.7248	899.7214	0.442985
0.8	2	80	35	45.04	60.066	903.7248	900.0704	0.40437
1	2	80	35	43.38	60.678	903.7248	900.8205	0.321369
1.2	2	80	35	42.15	61.106	903.7248	901.2219	0.276945
1.4	2	80	35	41.226	61.423	903.7248	901.6511	0.22946
1.6	2	80	35	40.5	61.667	903.7248	902.0057	0.190218
1.8	2	80	35	39.916	61.86	903.7248	902.2986	0.157806
2	2	80	35	39.441	62.016	903.7248	902.5707	0.127703

Table 2
Simulation error vs. mass flow rate ratio m

Me	m	t_3 (°C)	t_6 (°C)	t_4 (°C)	t_5 (°C)	Q_i (W)	Q_0 (W)	Error (%)
1.6	1	75	35	38.39	51.826	233.9648	545.7958	0.386729
1.6	1.5	75	35	39.37	56.399	233.9648	700.9586	0.557704
1.6	2	75	35	40.44	59.829	233.9648	858.5884	0.380147
1.6	2.5	75	35	41.56	62.495	233.9648	1,018.598	0.023729
1.6	3	75	35	42.69	64.624	233.9648	1,180.53	–0.40101
1.6	3.5	75	35	43.82	66.355	233.9648	1,343.889	–0.83278
1.6	4	75	35	44.94	67.78	233.9648	1,508.127	–1.23256

Table 3
Simulation error vs. temperature of spraying water t_3

Me	m	t_3 (°C)	t_6 (°C)	t_4 (°C)	t_5 (°C)	Q_i (W)	Q_0 (W)	Error (%)
1.2	2.5	65	35	42.56	57.1	233.9648	910.3181	0.423502
1.2	2.5	70	35	42.87	59.62	233.9648	962.9784	0.365889
1.2	2.5	75	35	43.07	61.87	233.9648	1,017.348	0.146397
1.2	2.5	80	35	43.18	63.882	233.9648	1,073.41	–0.20963

number. Fig. 11 depicts the impact of the spray water temperature on the Me number at a packing bed height of L = 1.2 m and an entering air temperature of 38°C. The experimental results reveal that, for a given value of m, the higher the spray water temperature, the lower the Me number. This phenomenon occurs because at high spray water temperatures, the thermal load on the device increases while the contact surface area remains constant. As a result, the efficiency of heat and mass transfer decreases, leading to a reduction in the Me number. The relationship between the Me number and the spray water temperature follows a non-linear curve, with significant variations in the Me number within the temperature range below 75°C. Additionally, at a constant spray water temperature, the Me number varies inversely with m. A higher mass flow ratio between spray water and air corresponds to a lower Me number. Furthermore, the change in the Me number tends to decrease slowly as m increases.

4.7. Effect of packing bed height on Me number

The height of the packing bed is a critical parameter that significantly influences the heat transfer and mass transfer in the humidifier. A taller packing bed results in a longer heat and mass transfer duration between water and air. However, the heat and mass transfer coefficients do not directly correlate with the packing bed height. Theoretical findings have revealed that as the Me number increases, the efficiency improvement of the humidifier slows down. Additionally, the resistance of the airflow passing through the packing bed also rises with the height of the packing bed. Hence, studying the impact of packing bed height on heat and mass transfer efficiency holds great importance.

To determine the mass transfer coefficients of the humidifier, it is necessary to first establish the heat transfer coefficients of both the air and water in the humidifier. However, the heat transfer coefficient between spray

water and air is influenced by various parameters, such as air velocity, water film velocity, humidifier height, packing bed material, and more. There is no general relationship for the mass transfer coefficient that accounts for the physical properties and specifications of the packing bed material. Consequently, the experimental approach is employed to determine the mass transfer coefficients for different types of packing bed materials.

The experimental results presented in Fig. 12 demonstrate that the Me number increases with an increase in the packing bed height. This can be easily understood by considering that an increase in the height of the packing bed enhances the transfer area, resulting in improved efficiency of heat and mass transfer, thus increasing the Me number. However, as the packing bed height becomes higher, the variation of the Me number with m tends to diverge.

The results in Figs. 11 and 12 both indicate that an increase in m leads to a decrease in the Me number. This aligns with the theoretical understanding that the Me number is inversely proportional to the spray water flow.

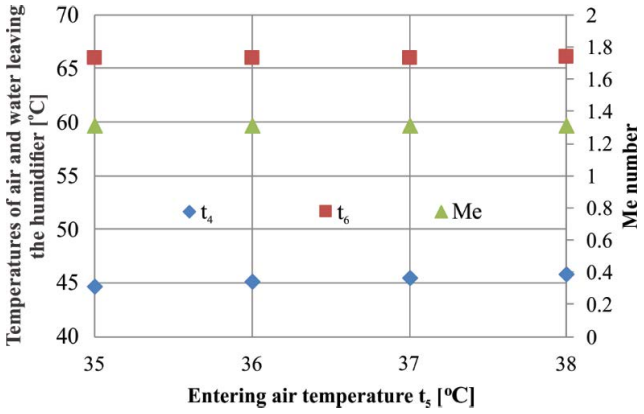

Fig. 10. Effect of entering air temperature on temperatures of air and water leaving the humidifier at t_3 = 75°C and m = 3.5.

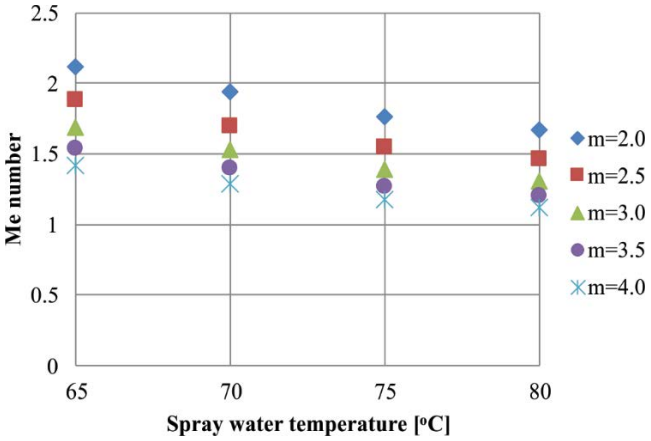

Fig. 11. Effect of spray water temperature and m to Me number.

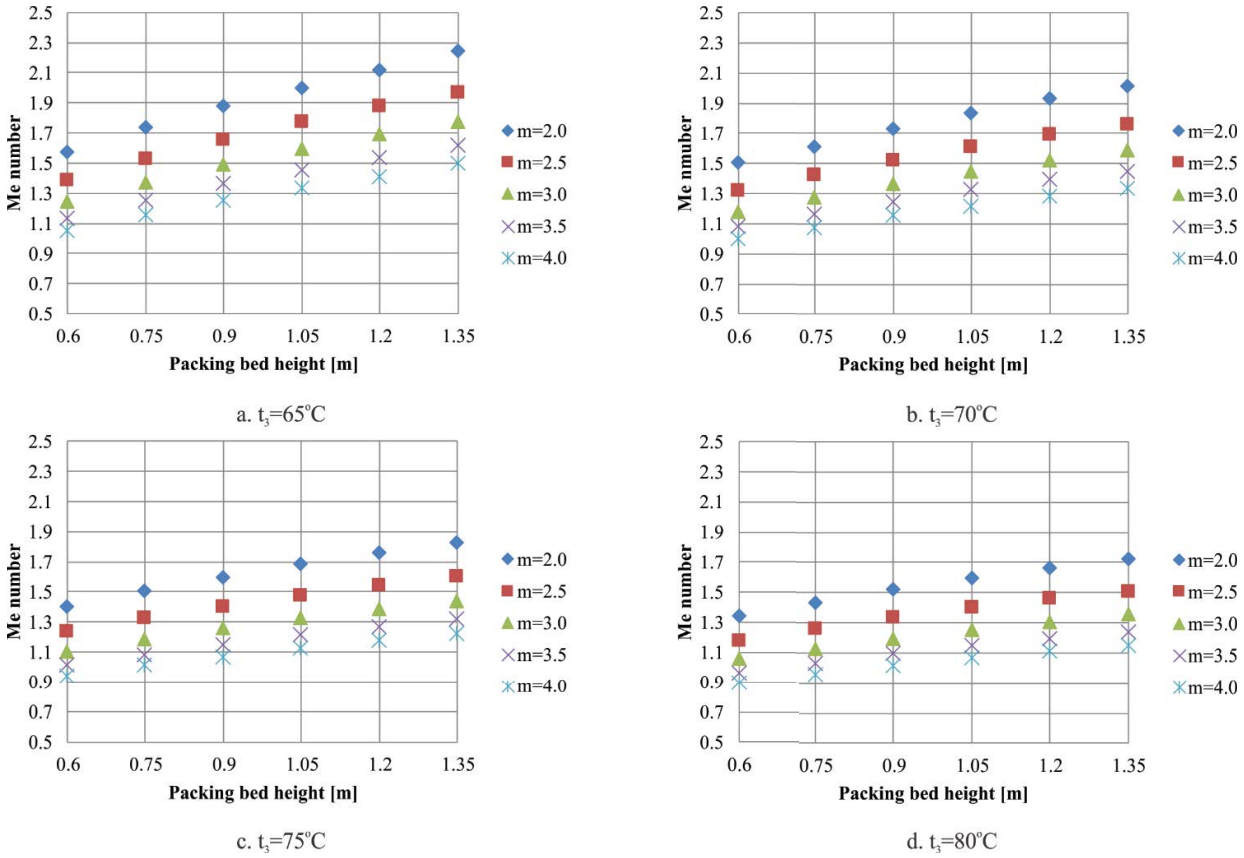

Fig. 12. Effect of packing bed height and m to Me number at t_5 = 35°C.

This can be further explained by the fact that as the spray water flow increases, the water density per unit contact area also increases, resulting in a decrease in heat and mass transfer efficiency.

From the experimental findings, it is evident that the performance of the humidifier depends solely on three crucial input parameters: the height of the packing bed layer, the mass flow rate ratio between water and air, and the temperature of the spray water.

Using the Statistical Package for the Social Sciences (SPSS) regression analysis software, the relationship of Me number with m, packing bed height and spray water temperature is built as follows:

$$\mathrm{Me} = \left(0.0012t^2 - 0.2174t + 11.933\right)m^{-0.583}L^{\left(0.0006t^2 - 0.0955t + 4.1097\right)} \quad (49)$$

Eq. (49) applies to the cooling pad paper material, the spray water temperature is in the range of 65°C–80°C and m is in the range of 1–4.

5. Conclusions

Based on theoretical and experimental study results on the process of heat and mass exchange between water and air in the humidifier, the following conclusions have been drawn:

- With a constant Me number and m, the temperature of water leaving the humidifier shows minimal variation with the spray water temperature. On the other hand, the temperature of the air leaving the humidifier exhibits a more significant difference depending on the spray water temperature. As m increases, both the temperatures of water and air leaving the humidifier also increase.
- As the Me number increases, the temperature of air leaving the humidifier will rise, while the temperature of water leaving the humidifier will decrease. For larger Me number and m values, the air temperature leaving the humidifier exhibits minimal changes with m. However, the temperature of water leaving the humidifier shows a notable difference. This demonstrates that higher m values may not be advantageous in terms of heat and mass transfer.
- As the Me number increases, the heat and mass transfer efficiency improve, but if the Me number becomes too large, the increase in heat and mass transfer efficiency becomes insignificant. Simulation results indicate that when Me > 1.6, the efficiency of heat and mass transfer experiences minimal change. Therefore, it is recommended to use a Me number value of 1.6 for designing the humidifier as it offers an appropriate balance between efficiency and practicality.
- The air temperature entering the humidifier has almost no effect on the Me number.
- Low spray water temperature and low mass flow ratio improve the efficiency of the humidifier.
- Based on experimental research using cooling pad paper as a packing bed material, a regression equation has been developed to depict the relationship between the Me number and spray water temperature, packing bed height, and m. This equation allows for easy determination of the appropriate packing bed size for the chosen Me and m, as well as the spray water temperature.
- The Me number is a specific parameter used to characterize mass transfer in humidifiers, particularly in direct contact cooling towers. However, the process of heat and mass transfer in direct contact heat exchangers is highly complicated. Determining the mass transfer coefficient requires experimental investigation due to the variations in characteristics among different packing bed materials. Using numerical simulation methods, the relationship between the spray water temperature, the temperature of air entering the humidifier, and the Me number with the temperatures of water and air leaving the humidifier has been established. This relationship enables the easy determination of the appropriate packing bed height in the design of the humidifier.

Acknowledgement

We acknowledge Ho Chi Minh City University of Technology (HCMUT), VNU-HCM for supporting this study.

Symbols

a	—	Surface area per unit volume, m^2/m^3
A	—	Area, m^2
Cp	—	Specific heat, J/kg·K
h	—	Enthalpy, J/kg
Le	—	Lewis factor, –
K_M	—	Mass transfer coefficient, kg/s·m^2
m	—	Mass flow rate ratio, –
$\dot{m}$	—	Mass flow rate, kg/s
Q	—	Heat transfer rate, W
r	—	Latent heat, kJ/kg
t	—	Temperature, °C
V	—	Volume of packing bed material, m^3
w	—	Moisture content, kg/kg

Greek

α	—	Convection coefficient, W/m^2·K
Δ	—	Difference

Subscripts

a	—	Air
i	—	In
o	—	Out
sa	—	Saturated air at temperature of spray water
v	—	Vapor
w	—	Water

Abbreviations

CAOW	—	Closed air open water
HDD	—	Humidification–dehumidification desalination
Me	—	Merkel number

References

[1] S. Hou, S. Ye, H. Zhang, Performance optimization of solar humidification–dehumidification desalination process using Pinch technology, Desalination, 183 (2005) 143–149.

[2] G.P. Narayan, M.H. Sharqawy, E.K. Summers, J.H. Lienhard, S.M. Zubair, M.A. Antar, The potential of solar-driven humidification–dehumidification desalination for small-scale decentralized water production, Renewable Sustainable Energy Rev., 14 (2010) 1187–1201.

[3] N.K. Nawayseh, M.M. Farid, A.A. Omar, S.M. Al-Hallaj, A.R. Tamimi, A simulation study to improve the performance of a solar humidification–dehumidification desalination unit constructed in Jordan, Desalination, 109 (1997) 277–284.

[4] M.M. Farid, S. Parekh, J.R. Selman, S. Al-Hallaj, Solar desalination with a humidification–dehumidification cycle: mathematical modeling of the unit, Desalination, 151 (2003) 153–164.

[5] J. Orfi, M. Laplante, H. Marmouch, N. Galanis, B. Benhamou, S.B. Nasrallah, C.T. Nguyen, Experimental and theoretical study of a humidification–dehumidification water desalination system using solar energy, Desalination, 168 (2004) 151–159.

[6] G. Al-Enezi, H. Ettouney, N. Fawzy, Low temperature humidification dehumidification desalination process, Energy Convers. Manage., 47 (2006) 470–484.

[7] R. Xiong, S. Wang, Z. Wang, A mathematical model for a thermally coupled humidification–dehumidification desalination process, Desalination, 196 (2006) 177–187.

[8] E.H. Amer, H. Kotb, G.H. Mostafa, A.R. El-Ghalban, Theoretical and experimental investigation of humidification–dehumidification desalination unit, Desalination, 249 (2009) 949–959.

[9] S. Farsad, A. Behzadmehr, Analysis of a solar desalination unit with humidification–dehumidification cycle using DoE method, Desalination, 278 (2011) 70–76.

[10] J.-J. Hermosillo, C.A. Arancibia-Bulnes, C.A. Estrada, Water desalination by air humidification: mathematical model and experimental study, Sol. Energy, 86 (2012) 1070–1076.

[11] M.H. Hamed, A.E. Kabeel, Z.M. Omara, S.W. Sharshir, Mathematical and experimental investigation of a solar humidification–dehumidification desalination unit, Desalination, 358 (2015) 9–17.

[12] J. Moumouh, M. Tahiri, M. Salouhi, L. Balli, Theoretical and experimental study of a solar desalination unit based on humidification–dehumidification of air, Int. J. Hydrogen Energy, 41 (2016) 20818–20822.

[13] B. Lacerda de Oliveira Campos, A. Oliveira Souza da Costa, K. Cecília de Souza Figueiredo, E. Ferreira da Costa Junior, Performance comparison of different mathematical models in the simulation of a solar desalination by humidification–dehumidification, Desalination, 437 (2018) 184–194.

[14] T. Ke, X. Huang, X. Ling, Numerical and experimental analysis on air/water direct contact heat and mass transfer in the humidifier, Appl. Therm. Eng., 156 (2019) 310–323.

[15] A.S.A. Mohamed, M.S. Ahmed, A.G. Shahdy, Theoretical and experimental study of a seawater desalination system based on humidification–dehumidification technique, Renewable Energy, 152 (2020) 823–834.

[16] M.A. Ahmed, N.A.A. Qasem, S.M. Zubair, Analytical and numerical schemes for thermodynamically balanced humidification–dehumidification desalination systems, Energy Convers. Manage., 200 (2019) 112052, doi: 10.1016/j.enconman.2019.112052.

[17] Y. Zhang, H. Zhang, W. Zheng, S. You, Y. Wang, Numerical investigation of a humidification–dehumidification desalination system driven by heat pump, Energy Convers. Manage., 180 (2019) 641–653.

[18] D. Kaunga, R. Patel, I.M. Mujtaba, Humidification–dehumidification desalination process: performance evaluation and improvement through experimental and numerical methods, Therm. Sci. Eng. Prog., 27 (2022) 101159, doi: 10.1016/j.tsep.2021.101159.

[19] S. Saidi, R. Ben Radhia, N. Nafiri, B. Benhamou, S.B. Jabrallah, Numerical study and experimental validation of a solar powered humidification–dehumidification desalination system with integrated air and water collectors in the humidifier, Renewable Energy, 206 (2023) 466–480.

[20] M. Poppe, H. Rogener, Berechnung von Ruckkuhlwerken, VDI-Warmeatlas, Mi 1–Mi 15 (1991).

[21] H. Ettouney, Design and analysis of humidification dehumidification desalination process, Desalination, 183 (2005) 341–352.

[22] A. Eslamimanesh, M.S. Hatamipour, Mathematical modeling of a direct contact humidification–dehumidification desalination process, Desalination, 237 (2009) 296–304.

[23] S.M. Soufari, M. Zamen, M. Amidpour, Performance optimization of the humidification–dehumidification desalination process using mathematical programming, Desalination, 237 (2009) 305–317.

[24] W.K. Lewis, The evaporation of a liquid into a gas, Trans. ASME, (1922) 325–340.

[25] F. Bosnjakovic, Technische Thermodinamik, 1965.

[26] F. Merkel, Verdunstungskühlung, VDI-Zeitchrift, 1925.

[27] K.Q. Vo, C.H. Le, A.Q. Hoang., Optimization of mass flow rate ratio of water and air in humidification–dehumidification desalination systems, Desal. Water Treat., 246 (2022) 82–91.